On the Linearity of Open Loop Fluxgate

İlker Yağlıdere[1,2] and Ece Olcay Güneş[1]

[1]Electronics and Communication Engineering Department, Istanbul Technical University, Istanbul, 34469, Turkey
iyaglidere@gmail.com, gunesec@itu.edu.tr
[2]ASELSAN Electronics Inc., 296. Street, 06370, Ankara, Turkey

Abstract

An open loop ring-core fluxgate sensor is designed. Measured sensor parameters and building steps are presented. The sensor is built on a crystalline core stacked from circular permalloy laminations. All electronic parts are designed. A control card is manufactured and used in the experiment. Several measurements are performed to investigate the open loop linearity. Although the upper linear measurement limit for open loop fluxgate is accepted as 1 μT in the literature, this study shows that open loop fluxgates can measure up to 15 μT without any special circuitry. We propose the upper linear measurement limit of an open loop fluxgate to be defined as a function of demagnetization factor instead of the conventionally accepted 1 μT value. This study shows that the measurement limit of an open loop fluxgate can be increased for a higher demagnetization factor at the expense of increased noise.

1. Introduction

Linearity is one of the most important parameters in fluxgate sensor design. Expensive high performance products are mostly operated in a closed loop configuration in which a compensation coil is used to produce an opposite field so that the sensor is always exposed to a "zero" field by the effect of the negative feedback [1]. However, low cost sensors used in shielded environments can be operated in an open loop configuration. Unfortunately, there are only a few number of studies, which investigate the open loop linearity of bulk type ring-core fluxgate. The well-known book [2] defines the upper measurement limit of open loop fluxgate as 1 μT. The measurement data from [3] point to a similar limit. The goal of this study is examining the upper measurement limit of open loop fluxgate in comparison with the literature.

2. Short-circuited Fluxgates

Current output fluxgates have been used since Primdahl implemented the first short-circuited fluxgate in 1989 by using a transimpedance amplifier [4]. They have a similar performance as compared to traditional voltage output fluxgates, except for the frequency response. The frequency response of the short-circuited fluxgate is superior and it is suitable for broadband operation due to the absence of the parasitic coil capacitance, which may cause resonance and measurement errors. Such a configuration was preferred in both Ørsted [5] and Astrid-2 [6] satellites.

In another study in 1991, Primdahl used a gated integrator to evaluate the fluxgate output current [7]. This mode does not only simplify the circuitry, but also uses the whole information from the even harmonics. In such electronics, the entire sensor performance is strongly correlated with the characteristics of the gating signal (e.g. gating width and phase delay) which should be adjusted experimentally with high precision.

In contrast to the voltage output approach, the sensitivity of current output fluxgate increases with the decreasing number of pickup coil turns. However, some mechanisms limit the minimum number of pickup coil windings. The sensitivity of a 17 mm toroidal core sensor can reach 40 nA/nT while a similar voltage output fluxgate can reach 20 μV/nT [2].

In this work, the short-circuited fluxgate followed by a gated integrator is used. Ring-core geometry is preferred due to its high signal-to-noise ratio. The ring-core offers perfect symmetry and in this way, the pickup coil is highly isolated from the excitation coil.

3. Sensor Design and Fabrication

The fluxgate core is stacked from four circular 1J85 permalloy laminations and physical dimensions of the sensor are tabulated in the Table 1. Some mechanical details are shown in Fig. 1 and production steps are illustrated in Fig. 2. Mechanical design (a, c), main frame production with plastic molding technique (b, e), stacked core production from ring laminations (d, e) and final sensor assembly with windings (f) are the key steps in the production. In the configuration used, the toroidal core close fits to the support material and the structure is mechanically stable. For this reason, the structure used is suitable for commercial sensors.

Table 1. Sensor dimensions

Parameter	Symbol	Unit (mm)
lamination thickness	$t_{lamination}$	0.3
outer diameter (bare)	OD_{bare}	12.17
inner diameter (bare)	ID_{bare}	8.81
height (bare)	h_{bare}	1.20
outer diameter (boxed)	OD_{boxed}	13.65
inner diameter (boxed)	ID_{boxed}	7.70
height (boxed)	h_{boxed}	2.80
excitation coil wire diameter	d_{exc}	0.12
pickup coil wire diameter	d_{pickup}	0.40
pickup coil length	l_{pickup}	15.10
pickup coil width	w_{pickup}	20.00
pickup coil height	h_{pickup}	5.0

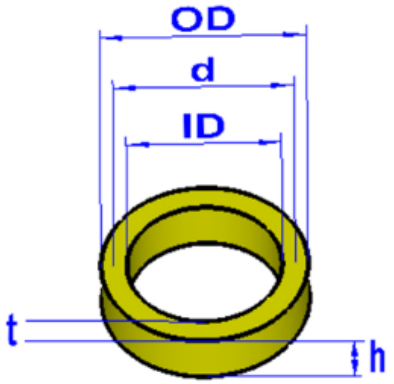

Fig. 1. Dimensions of the ring-core

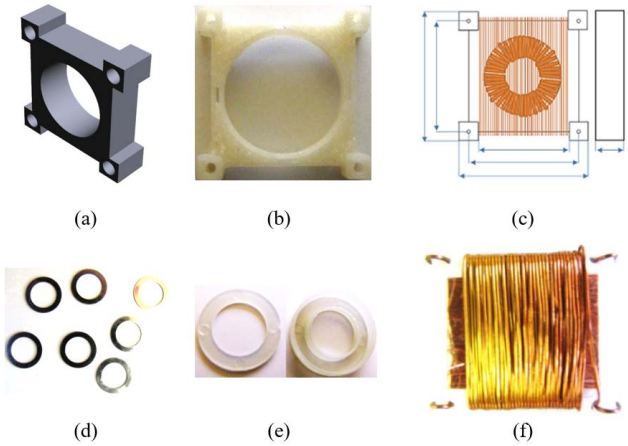

Fig. 2. Production steps of the designed sensor, from mechanical design to physical sensor production: (a, b, c) mechanical design, (d) permalloy laminations, (e) plastic case for laminations, (f) ready-to-use finished sensor

Fig. 3. Control card designed for the experiment

4. Sensor Electronics

The designed control card shown in Fig. 3 performs all analog signal processing as well as producing the excitation current for the sensor. The sensing circuitry is given in Fig. 4. Processed analog sensor current is digitized through the analog-to-digital converter embedded in the digital signal processor.

Drive circuitry is composed of an H bridge, which contains complementary MOSFETs. PWM (Pulse Width Modulation) signals and synchronous gating clock are generated with the digital signal processor. High side and low side control signals for each half bridge are generated as complementary signals with some dead time to prevent shot-through. Schottky diodes are also used in antiparallel to parasitic junction diodes, for protection against the instantaneous coil voltage. No resonant capacitors are used for both excitation and sensing coils since it would increase the temperature dependency of the system. The excitation coil is excited with 1 kHz square wave voltage, which provides 2000 current pulses in each second. Excitation current pulses with a peak value of 0.47 A in each direction saturate the core deeply as well as serving to decrease the noise and perming effect. The resulting excitation current waveform is shown in Fig. 5a.

In the analog front-end, a 150 Ω gain transimpedance preamplifier followed by a gated integrator with 30x gain in the passband is used for signal extraction. Actually, the first stage shown in Fig. 4 forms an inverting amplifier with 555x gain, when combined with the 0.27 Ω parasitic sensing coil resistance. Special care should be taken with such a high gain while using operational amplifiers. The high gain-bandwidth product of OP37 allows high gain amplification in the frequency range of interest. The gating function provides selective integration by blocking the spurious signals outside the fluxgate signal frame and serves to decrease the noise. The resulting waveform after the gating function is a spurious-free signal, which is shown in Fig. 5c, and it is quite different from the original waveform given in Fig. 5b.

5. Measurements and FEM Analysis

The system operates with two supply voltages (±5 V). Some calculation, measurement and FEM (Finite Element Method) analysis results are tabulated in Table 2. Overall system specifications are summarized in Table 3.

The waveforms for 14 μT external magnetic field are given in Fig. 5. Global demagnetization factor is measured as 0.0395. Some details on measuring the factor are given in [8]. To validate the measurement result, a finite element analysis is performed with CST EM Studio and it results in a similar value,

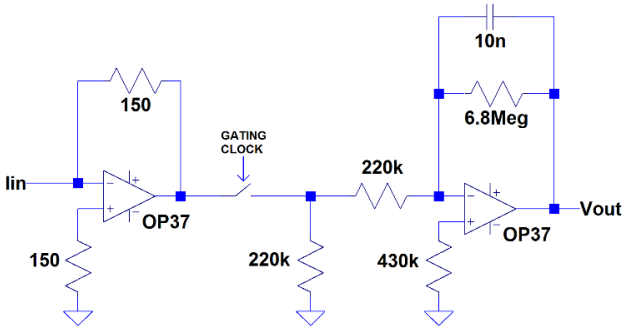

Fig. 4. Sensing electronics

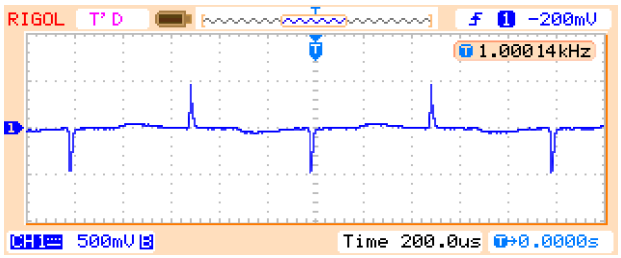

(a) excitation current measured via 1 Ω

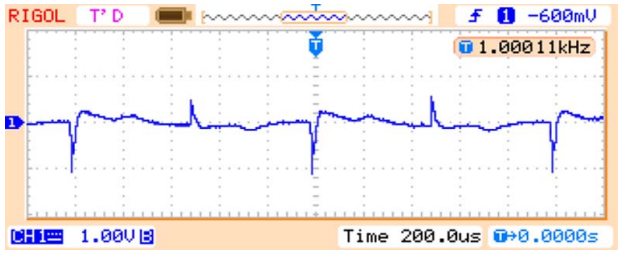

(b) resulting pickup coil current x 150 Ω

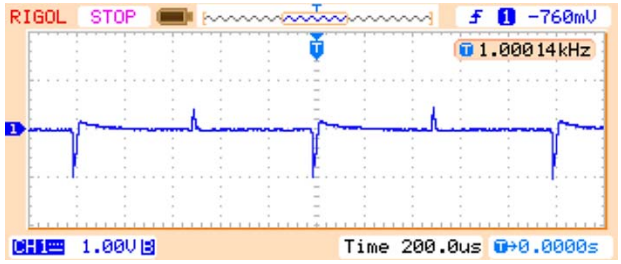

(c) gated signal

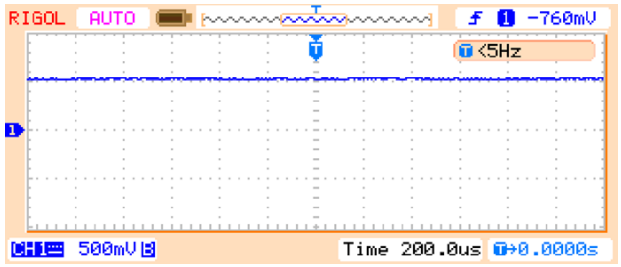

(d) integrated signal used as the sensor output voltage

Fig. 5. Current and voltage waveforms for 14 µT external field

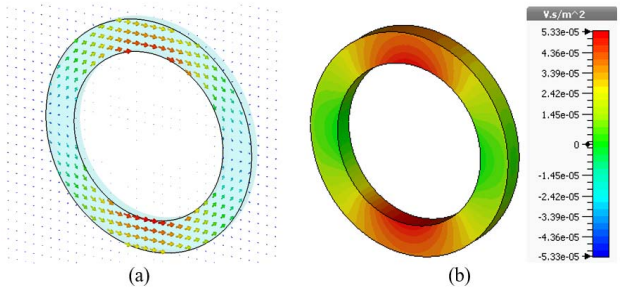

(a) (b)

Fig. 6. (a) B-field vector plot and (b) color map of B-field magnitude in the measurement axis under the influence of an external field

Table 2. Sensor parameters

Parameter	Symbol	Unit	Value
material	-	-	permalloy 4 laminations
path length	l_{path}	mm	32.67
core cross sectional area	A_{core}	mm^2	2.016
relative core permeability	μ_r	-	~20000[a]
demagnetization factor	D	-	0.0395[a] 0.0440[b]
excitation winding number	N_{exc}	turns	160
excitation coil resistance	R_{exc}	Ω	3.4[a]
excitation coil inductance	L_{exc}	mH	53.35[a]
pickup winding number	N_{pickup}	turns	36
pickup cross sectional area	A_{pickup}	mm^2	100
pickup coil resistance	R_{pickup}	Ω	0.27[a]
pickup coil inductance	L_{pickup}	µH	18.00[a]

[a]measured
[b]FEM analysis result

Table 3. Sensor system specifications

Parameter	Value
open loop measurement range	±15 µT
output voltage sensitivity	40 mV/ µT
power consumption	19 mA @ +5 V, 2.5 mA @ -5 V

0.0440. The field distribution maps from the FEM analysis are given in Fig. 6.

6. Linearity Analysis

System response is analyzed by performing several measurements and the results are illustrated in Fig. 7. The figure shows that the designed system can measure the field density up to 15 µT without compensation and specific circuitry. The linearity error at 15 µT is about 6%. Above 15 µT, the output voltage starts to saturate and the linearity is lost.

Although 6% error level is an unacceptably high nonlinearity for a closed-loop fluxgate, it is a good and admissible value for an open loop fluxgate operating at the edge of its measurement limit. Therefore, the upper measurement limit for the designed sensor is determined as 15 µT. It can be possible to measure fields up to 100 µT by adding a feedback network to the system, but the closed-loop method increases the cost and power consumption.

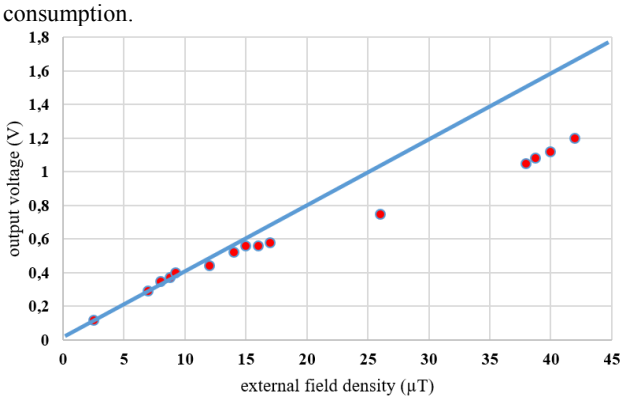

Fig. 7. The open loop fluxgate linearity analysis

7. Discussion and Conclusions

In this study, a short-circuited open loop fluxgate sensor system with low power consumption is designed to measure static and low frequency magnetic fields. Linearity of the permalloy core sensor is investigated. The upper measurement limit for an open loop fluxgate is given as 1 μT in the literature. However, the measurement results show that the open loop fluxgate can be operated up to 15 μT field density without any special circuitry. The designed sensor has a low diameter and a high thickness, which results in a high demagnetization factor measured as 0.0395. This value is found to be reliable because it is validated by a FEM analysis by using CST EM Studio. The increase in the linearity limit is probably caused by this high demagnetization factor, which results in blocking the external field to penetrate inside the core.

It is known that the sensitivity of fluxgate decreases for an increasing demagnetization factor. When the literature is reviewed, it is clear that most of the ring core fluxgates have a demagnetization factor value between 0.002 and 0.006, which corresponds to an average factor of 0.004. Since the demagnetization factor measured in this study (0.0395) is ten times of the average, approximately ten times increase in the linear measurement range is found to be meaningful.

In conclusion, we propose the upper measurement limit of open loop fluxgate to be defined as a function of demagnetization factor instead of a constant value.

8. Acknowledgment

Electromagnetic field simulation (FEM analysis) subsection of this research was supported by Aktif Neser Elektronik Ltd. Sti. and CST - Computer Simulation Technology AG by supplying a demo license for CST EM Studio.

9. References

[1] İ. Yağlıdere, “A Sensitive Fluxgate Magnetic Sensor Design”, M.S. thesis, Elec. and Com. Eng. Dept., Istanbul Tech. Univ., Istanbul, TR, 2010.

[2] P. Ripka, “Magnetic Sensors and Magnetometers”, Artech House, Boston, USA, 2001.

[3] P. Ripka, "Contribution to the ring-core fluxgate theory", *Phys. Scripta*, vol. 40, no. 4, pp. 544, Aug., 1989.

[4] F. Primdahl, et al., “The short-circuited fluxgate output current”, *J. Phys. E*, vol. 22, no. 6, pp. 349, Jun., 1989.

[5] O. V. Nielsen, et al., “Development, construction and analysis of the 'OErsted' fluxgate magnetometer”, *Meas. Sci. Technol.*, vol. 6, no. 8, pp. 1099, Aug., 1995.

[6] E. B. Pedersen, et al., “Digital fluxgate magnetometer for the Astrid-2 satellite”, *Meas. Sci. Technol.*, vol. 10, no. 11, pp. N124, Nov., 1999.

[7] F. Primdahl, P. Ripka, J. R. Petersen and O. V. Nielsen, "The short-circuited fluxgate sensitivity parameters", NASA STI/Recon Technical Report, N 92, Feb., 1991.

[8] F. Primdahl, et al., “Demagnetising factor and noise in the fluxgate ring-core sensor”, J. Phys. E, vol. 22, no. 12, pp. 1004, Dec., 1989.